

# Experimental Correlation for Splashing Condition of Droplets on Solid Substrates

Yukihiro Yonemoto <sup>1,\*</sup>, Kanta Tashiro <sup>2</sup>, Minori Yamashita <sup>2</sup> and Tomoaki Kunugi <sup>3,\*</sup>

<sup>1</sup> Division of Industrial Fundamentals, Faculty of Advanced Science and Technology, Kumamoto University, 2-39-1, Kurokami, Chuo-ku, Kumamoto-shi, Kumamoto, 860-8555, Japan

<sup>2</sup> Department of Mechanical and Mathematical Engineering, Kumamoto University, 2-39-1, Kurokami, Chuo-ku, Kumamoto-shi, Kumamoto, 860-8555, Japan; 202d3118@st.kumamoto-u.ac.jp (K.T.); 213d8529@st.kumamoto-u.ac.jp (M.Y.)

<sup>3</sup> College of Energy Engineering, Zhejiang University, 38 Zheda Road, Hangzhou, Zhejiang Province 310027, China

\* Correspondence: yonemoto@mech.kumamoto-u.ac.jp (Y.Y.); kunugi.tomoaki.85s@st.kyoto-u.ac.jp (T.K.)

## S1. Evaluation for the impingement velocity of droplets.

The impact velocity of droplets is measured from the captured images as shown in Figure S1.

The image at  $t_0$  [s] (Figure S1(a)) is set as a standard image for subsequent images from (b) to (e). The positions of the top of the droplet  $h_{t0}$  [m] and the bottom of the droplet  $h_{b0}$  [m] are initially determined. Then, the top and bottom positions of  $h_{ti}$  and  $h_{bi}$  ( $i = 1, \dots, n$ ) during time evolution are measured. From the data, the displacement for each position is calculated as follows:

$$\Delta h_j = h_{t0} - h_{tj}, \quad (j = 0, \dots, n) \quad (S1)$$

and

$$\Delta h_{bj} = h_{b0} - h_{bj}, \quad (j = 0, \dots, n) \quad (S2)$$

In a similar way, the time evolution is also calculated as follows:

$$\Delta t_j = t_j - t_0, \quad (j = 0, \dots, n) \quad (S3)$$

From Equations (S1) and (S2), the displacement of the middle position between top and bottom is calculated by a simple averaging procedure as follows:

$$\Delta h_{mk} = \frac{\Delta h_{tk} + \Delta h_{bk}}{2}, \quad (k = 0, \dots, n) \quad (S4)$$

The relationship between the calculated values for  $\Delta h_m$  (Equation (S4)) and  $\Delta t$  (Equation (S3)) are fitted by the following relation:

$$\Delta h_m = k_1 (\Delta t)^2 + k_2 \Delta t + k_3 \quad (S5)$$

In Equation (S5),  $k_1$ ,  $k_2$ , and  $k_3$  are fitting parameters. From the differentiation of Equation (S5) by  $\Delta t$ , the following relation is obtained:

$$u = 2k_1 \Delta t + k_2 \quad (S6)$$

By substitution of  $\Delta t = \Delta t_n$  into Equation (S6), the impact velocity  $u_{imp}$  [m/s] can be obtained.

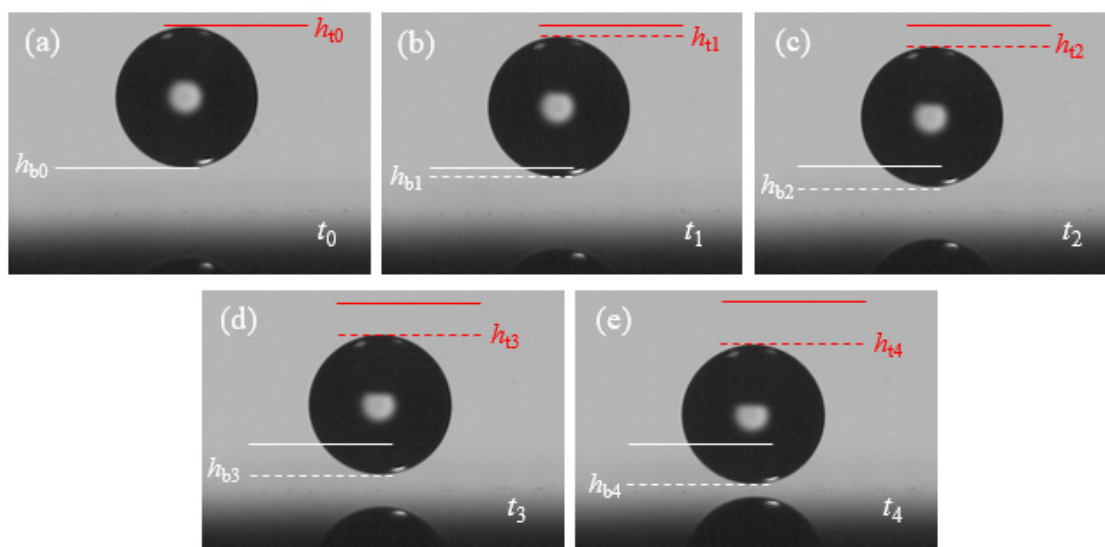


**Figure S1.** Images for determination of impingement velocity of droplets. The time advances from (a) to (e).

Figure S2 shows an example for the comparison of the relationship between the impingement velocity and analytical result of 99.4 wt% ethanol droplets ( $d_0 = 2.10 \times 10^{-3}$  [m]). The analytical result was calculated by the following equation [33]:

$$u = \sqrt{\frac{g}{k} [1 - \exp\{2k(d_0 - z)\}]} \quad (S7)$$

where  $g$  and  $z$  are the gravitational acceleration [ $\text{m/s}^2$ ] and release height [m], respectively.  $k$  is defined as  $(3/4)(\rho_{\text{air}} C_d)/(\rho d_0)$  in which  $\rho_{\text{air}}$  and  $C_d$  represent the density of the air and the drag coefficient, respectively. In the present study, the values of  $\rho_{\text{air}}$  and  $C_d$  are  $1.2$  [ $\text{kg/m}^3$ ] and  $0.47$  [-], respectively. The measured impingement velocities agree well with the analytical result evaluated by Equation (S7).

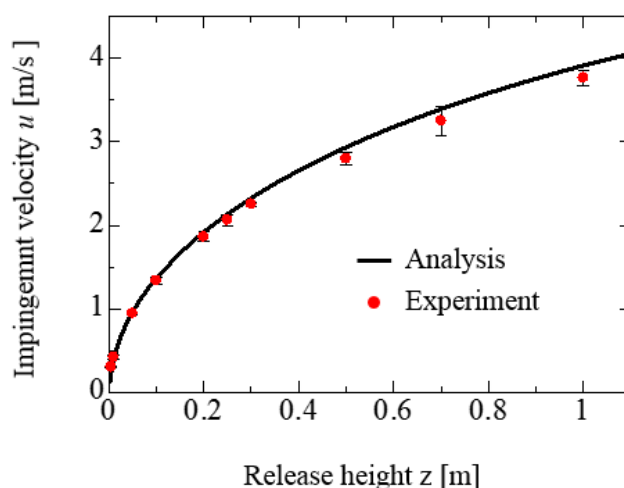


**Figure S2.** Comparison of measured impingement velocity of droplets with analytical results.

## S2. Coefficients in Equations (4), (5), (12), and (16).

### $f_{\text{rf}}$ dependency of the coefficients in Equations (5), (12), and (16).

In the present study, the effect of the surface roughness on the splashing condition was considered in Equations (5), (12), and (16). The values for the coefficients were obtained by fitting the experimental data with the equation. The wettability of droplets on solid substrate is basically characterized by relative relation among solid substrates [34]. Therefore, the surface roughness dependencies of the coefficients can be evaluated by considering the reference substrate. In the present study, the bare substrate was set as the reference substrate. For example, in Equation (5), the relationship between the coefficient  $(a - a_{\text{bare}})/a_{\text{bare}}$  and  $(f_{\text{rf}} - f_{\text{bare,rf}})/f_{\text{bare,rf}}$  was considered. Here, Figure S3 shows the  $f_{\text{rf}}$  dependency of the coefficients  $a$  and  $b$  in Equation (5). In this figure, the black solid circles represent the experimental values with the error bar. In both figures, as the  $f_{\text{rf}}$  increases, it is found that the coefficient approaches a certain constant value in each figure. These tendencies for each coefficient are well fitted by Equation (6) for  $a$  and Equation (7) for  $b$ , respectively. The values of  $C_{a1}$ ,  $C_{a2}$ ,  $C_{b1}$ , and  $C_{b2}$  in Equations (6) and (7) are determined by minimizing the differences between the experimental and predicted values for  $a$  and  $b$  with the multi-variable least square method. The red solid circles represent the predicted values and well reproduce the experimental values. The coefficients in Equations (12) and (16) were also considered in a similar manner. Figures S4 and S5 show the  $f_{\text{rf}}$  dependency of the coefficients of  $E$  and  $F$  in Equation (12) and  $G$  and  $H$  in Equation (16), respectively. All the predicted values well reproduce the experimental values in  $E$ ,  $F$ ,  $G$ , and  $H$ .

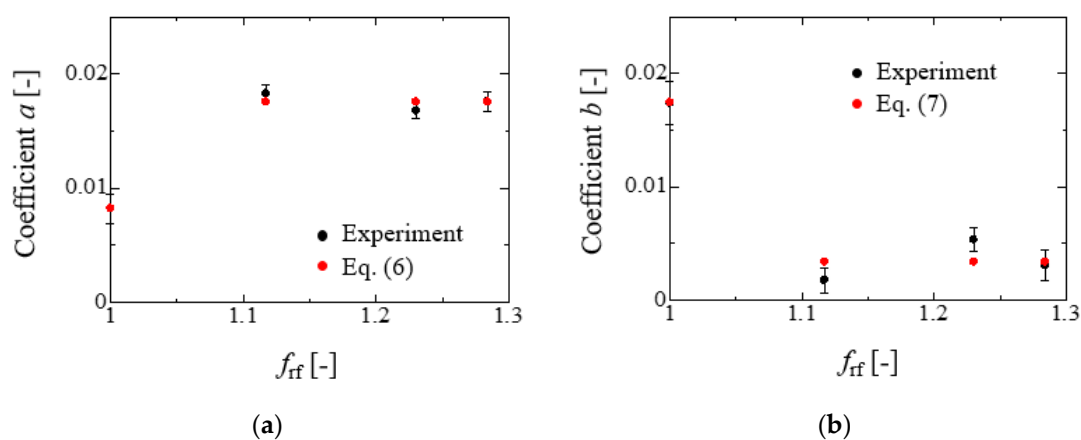


**Figure S3.** Relationship between the experimental and the predicted values for the coefficient  $a$  and  $b$  in Equation (5): (a)  $a$  vs  $f_{\text{rf}}$ ; (b)  $b$  vs  $f_{\text{rf}}$ .  $a$  and  $b$  are predicted by Equations (6) and (7), respectively.

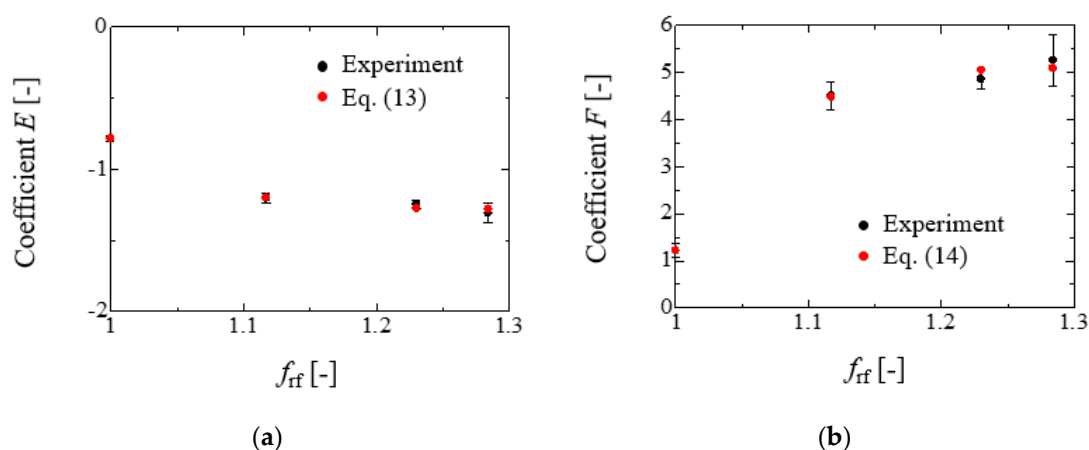


**Figure S4.** Relationship between the experimental and the predicted values for the coefficient  $E$  and  $F$  in Equation (12): (a)  $E$  vs  $f_{rf}$ ; (b)  $F$  vs  $f_{rf}$ .  $E$  and  $F$  are predicted by Equations (13) and (14), respectively.

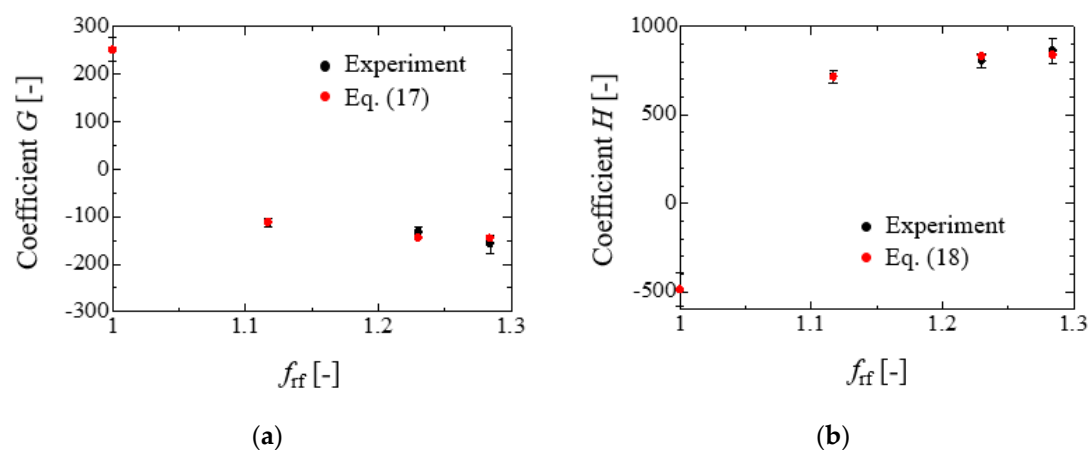


**Figure S5.** Relationship between the experimental and the predicted values for the coefficient  $G$  and  $H$  in Equation (16): (a)  $G$  vs  $f_{rf}$ ; (b)  $H$  vs  $f_{rf}$ .  $G$  and  $H$  are predicted by Equations (17) and (18), respectively.

### Coefficients in Equation (4)

Equation (4) originally considers the effect of the surface roughness on the splashing condition as  $\ln(R_a/d_0)$ . The liquid properties are also considered in the coefficients  $C$  and  $D$  in Equation (4). However, the effect of the droplet volume on each coefficient was not considered in the original work [33]. Therefore, the formulation of the coefficients  $C$  and  $D$  are performed focusing on the droplet size dependency. For example, Figure S6 shows the droplet size dependency of each coefficient for the case of 70 wt%. As shown in Figure 9(c), the coefficients  $C$  and  $D$  for each droplet size of Figure S6 are obtained from the three linear fitting lines for the relationship between  $K_t$  and  $\ln(R_a/d_0)$ . From Figure S6, it is found that the coefficient  $C$  exhibits the droplet size dependency, while the coefficient  $D$  takes an almost constant value. Similar treatment was performed for other liquid cases. Here, the parameter  $K_t (= (We/Oh)^{1/2})$  of Equation (4) can be alternatively represented by the expression  $(ReFr)^{1/2}(d_0/l_{cap})^{1/2}$ ,  $Fr (= u/(gd_0)^{1/2})$  is Froude number. Therefore, the parameter  $(d_0/l_{cap})^{1/2}$  can also be an important factor to determine the parameter  $K_t$ . In addition, the coefficient  $C$  exhibited the droplet volume dependency. Therefore, the coefficient  $C$  was divided by  $(d_0/l_{cap})^{1/2}$  as shown in Figure 10(a). The averaged values of  $C/(d_0/l_{cap})^{1/2}$  and  $D$  exhibit a potential for the correlation of  $\alpha Oh_{cap}^n + \beta$  as shown in Figures. 10(c) and (d). Finally, the coefficients  $C_1$ ,  $C_2$ ,  $D_1$ ,  $D_2$ , and the exponent of  $Oh_{cap}$  are determined by minimizing the differences in the experimental and calculated values of  $K_t$  with the multivari-

able least square method. Figure S7 shows the comparison of the experimental and predicted values for the coefficient  $C$  divided by  $(d_0/l_{cap})^{1/2}$  and  $D$ . The predicted value shows agreement with the experimental value within the error.

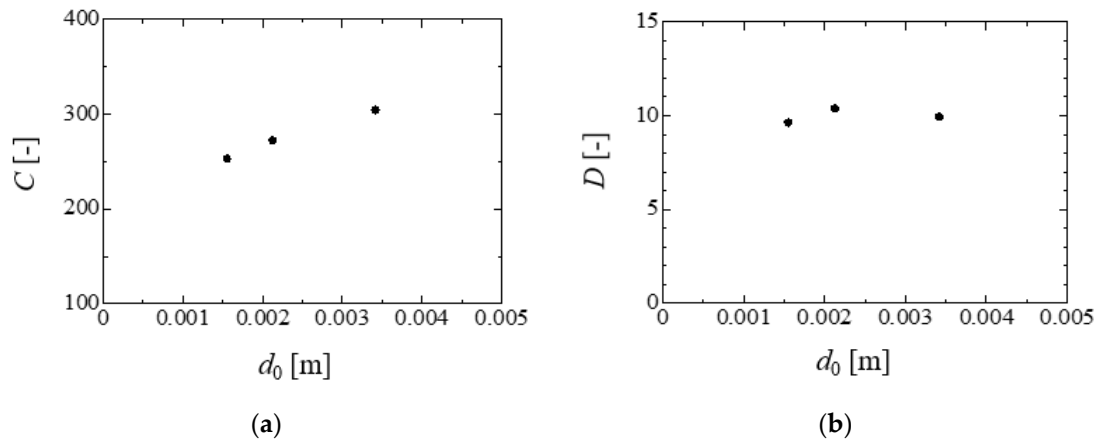


**Figure S6.** Example for droplet size dependency of the coefficients  $C$  and  $D$  in Equation (4) for the case of 70 wt%: (a)  $C$  vs  $d_0$ ; (b)  $D$  vs  $d_0$ .

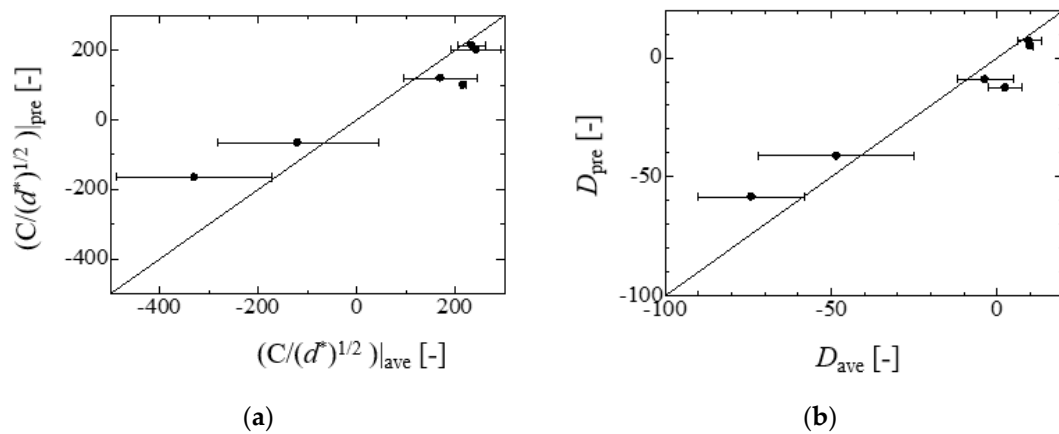


**Figure S7.** Comparison of experimental and predicted values: (a) coefficient  $C$  divided by  $(d_0/l_{cap})^{1/2}$ ; (b) coefficient  $D$ .